A DIDACTIC COMPARISON OF SPACE-VECTOR PWM AND CARRIER-BASED PWM WITH OPTIMAL ZERO-SEQUENCE INJECTION

Wilson Komatsu Lourenço Matakas Jr.

Escola Politécnica da Universidade de São Paulo, Av. Prof. Luciano Gualberto, trav. 3, no. 158, 05508-900
São Paulo SP, BRAZIL
email: matakas@pea.usp.br

Abstract: **A didactic comparison of space-vector PWM and carrier-based PWM with optimal zero-sequence injection, is presented. The optimality of the Space Vector PWM regarding current ripple is emphasized. Both methods are compared in time domain and space vector domain.**

Keywords: **Carrier-Based PWM, Education in Power Electronics, Optimal Space-Vector PWM, Zero-Sequence Injection.**

I.INTRODUCTION

Space-vector PWM (SVPWM) and carrier-based PWM (CPWM) are largely used in PWM controlled converters. The SVPWM is well known for its low current ripple, ability to supply larger output voltages for a given DC link, and convenience to be used together with space vector based higher level control loops. The CPWM is simple, and is easily implemented by the PWM blocks available in the dedicated DSPs and micro controllers, requiring no additional computational load. Although it is possible to obtain exactly the same behavior of a SVPWM, by using the CPWM with zero sequence injection at the reference inputs, there are still some misunderstandings that make people believe that the SVPWM is better than the CPWM. This summary describes the CPWM, its spectra, and two possibilities of zero sequence references: one that emulates SVPWM and other that minimizes a cost function based on the RMS value of the current ripple. The optimal behavior of the SVPWM regarding current ripple is confirmed. SVPWM and CPWM are explained and compared in time domain and Space Vector domain, deepening the understanding of both methods.

II. THREE-PHASE, THREE-WIRE CONVERTER AND ITS MODELING

A three-phase, three-wire (3P3W) converter (Fig. 1(a)) can be modeled as a wye connection of three ideal voltage sources (Fig. 1(b)), with no external access to the common point G1. Each voltage source corresponds to a half bridge (HB), two level ($\pm V_d$) converter.

Fig. 2(a) shows a balanced generic load connected to the 3P3W converter. Notice that common points G1 and G2 are not interconnected. As the HB converter can only present $+V_d$ or $-V_d$ at its terminals (v_c voltage, Fig. 1b), the instantaneous sum of the phase voltages of the 3P3W converter is not null ($v_{cr}(t)+v_{cs}(t)+v_{ct}(t)\neq 0$ (1)) and this fact apparently imposes difficulties for calculating the line currents $i_r(t)$, $i_s(t)$ and $i_t(t)$.

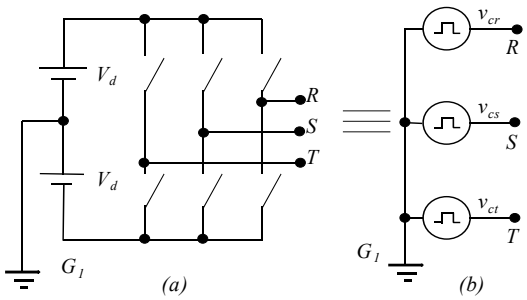

Fig. 1: (a) Half-bridge converter with split DC voltage source; (b) three-phase, three-wire converter representation of (a) as three ideal voltage sources.

One can define the instantaneous zero-sequence voltage $v_0(t)$ (2) and subtract it from each one of the phase voltages

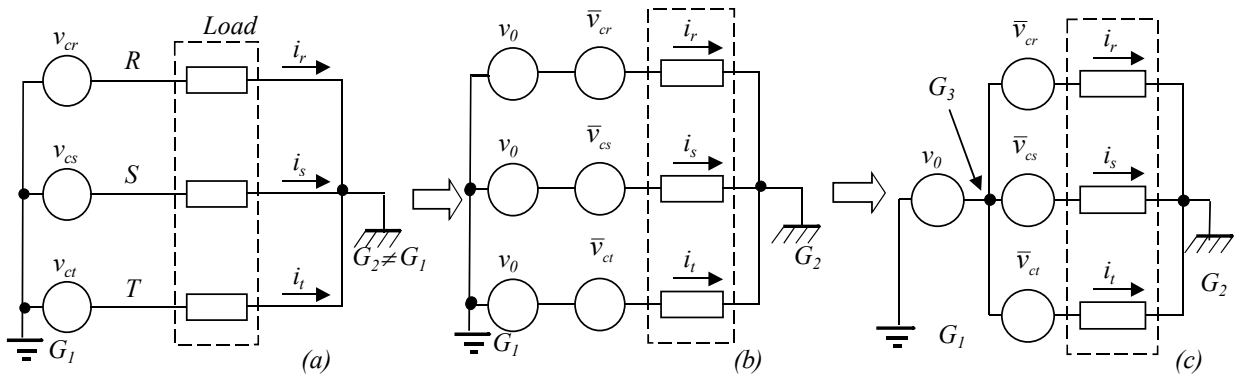

Fig. 2: (a) Balanced generic load connected to the 3P3W converter; (b) instantaneous zero-sequence voltage added to the new equivalent phase voltages; (c) equivalent circuit of (b).

$v_{cr}(t)$, $v_{cs}(t)$ and $v_{ct}(t)$, resulting the voltages $\bar{v}_{cr}(t)$, $\bar{v}_{cs}(t)$ and $\bar{v}_{ct}(t)$ (Fig. 2(b)). Notice that the sum of the resulting new phase voltages $v_{cr}(t)$, $v_{cs}(t)$ and $v_{ct}(t)$ is zero (3).

$$v_0(t) = \frac{v_{cr}(t) + v_{cs}(t) + v_{ct}(t)}{3} \quad (2)$$

$$\bar{v}_{cr}(t) + \bar{v}_{cs}(t) + \bar{v}_{ct}(t) = (v_{cr}(t) - v_0(t)) + (v_{cs}(t) - v_0(t)) + (v_{ct}(t) - v_0(t)) = 0 \quad (3)$$

Fig. 2(b) can be redrawn as Fig. 2(c), producing a new common point G3. If the load is balanced, it can be proved that the voltage between points G2 and G3 is null ($v_{G2G3}(t) = 0$ (4)) and the equivalent phase voltages $\bar{v}_{cr}(t)$, $\bar{v}_{cs}(t)$ and $\bar{v}_{ct}(t)$ impose currents $i_r(t)$, $i_s(t)$ and $i_t(t)$ to the load. As G1 and G2 are not connected, there is no current between them and the instantaneous zero-sequence $v_0(t)$ does not impose any current.

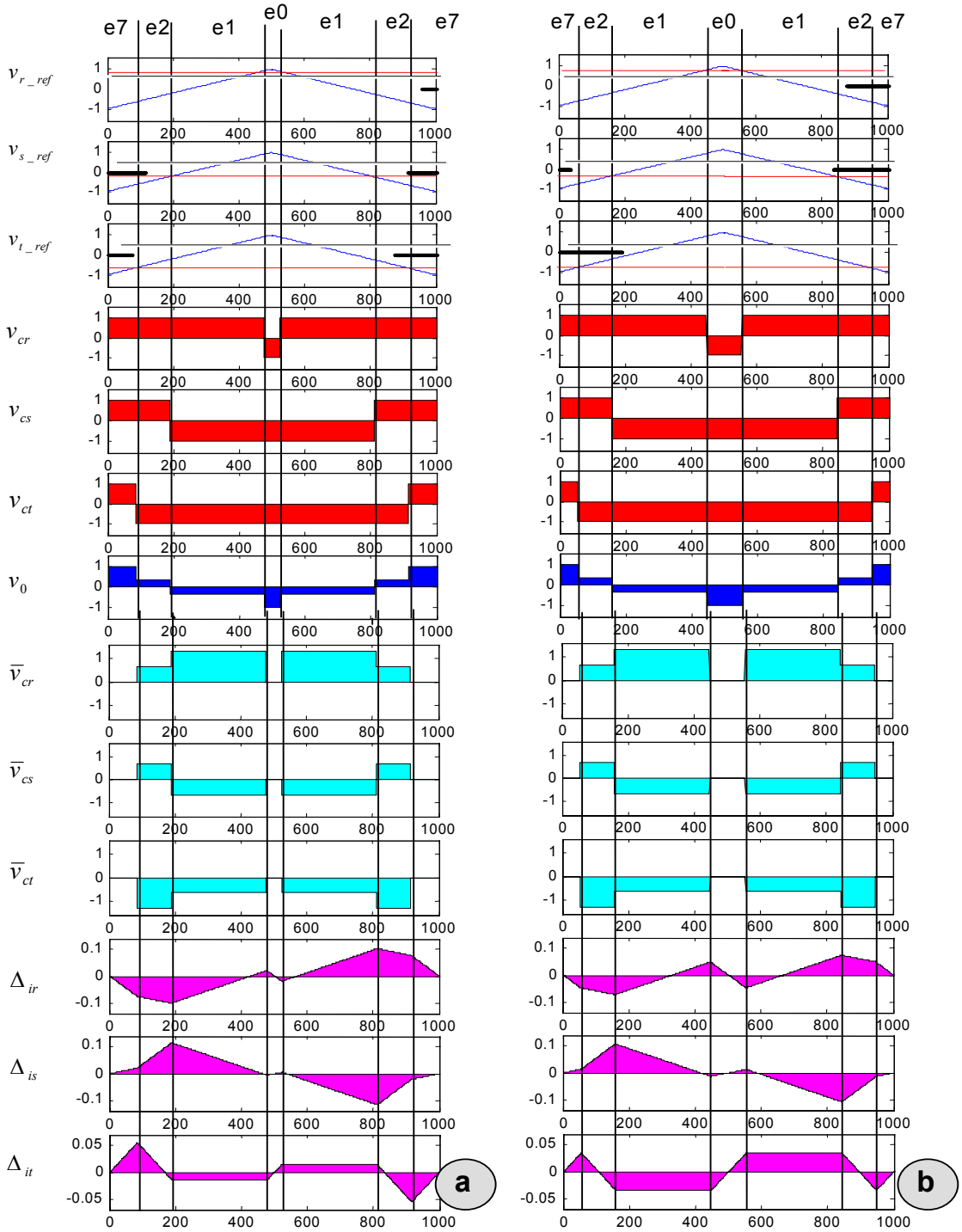

Fig. 3: Simulated waveforms for a CPWM applied to a 3P3W circuit, showing one PWM cycle (T_S): (a) with arbitrary values of references $v_{r\,ref}(t)$, $v_{s\,ref}(t)$ and $v_{t\,ref}(t)$, converter voltages $v_{cr}(t)$, $v_{cs}(t)$ and $v_{ct}(t)$, equivalent voltages $v_{cr}(t)$, $v_{cs}(t)$ and $v_{ct}(t)$, current ripple $\Delta i_r(t)$, $\Delta i_s(t)$, $\Delta i_t(t)$; (b) same signals of (a), adding $v_{0\,ref}(t)$, to the references (references shown as red lines).

III. CARRIER BASED PWM

Figs. 3(a) and 3(b) show some simulated waveforms for one carrier period T_S, where one considers that the references $v_{r\_ref}(t)$, $v_{s\_ref}(t)$ and $v_{t\_ref}(t)$ variation can be neglected (their values can be considered constant during T_S). The same triangular carrier was used for the three phases. Fig. 3(b) shows the result of summing an arbitrary instantaneous zero-sequence voltage reference $v_{0\_ref}(t)$ (also constant within T_S) to the original references $v_{r\_ref}(t)$, $v_{s\_ref}(t)$ and $v_{t\_ref}(t)$ of Fig. 3(a). In both Figs. 3(a) and 3(b), the sum of $v_{r\_ref}(t)$, $v_{s\_ref}(t)$ and $v_{t\_ref}(t)$ is null. The addition of $v_{0\_ref}(t)$ modifies the waveforms and the local average values of phase voltages $v_{cr}(t)$, $v_{cs}(t)$ and $v_{ct}(t)$, (the local average value of a signal can be defined here as its average value measured in a period equal to T_S). By the other side, the local average values of equivalent phase voltages $\overline{v}_{cr}(t)$, $\overline{v}_{cs}(t)$ and $\overline{v}_{ct}(t)$ do not change. Fig. 3 shows that the shape of the non-zero parts of their waveforms $\overline{v}_{cr}(t)$, $\overline{v}_{cs}(t)$ and $\overline{v}_{ct}(t)$ do not change with $v_{0\_ref}(t)$ injection, but they only slide along the time axis, changing the time intervals corresponding to the states e_0 and e_7 (Fig. 3, top). Time intervals corresponding to the states e_1 and e_2 do not change. The local average values of currents $i_r(t)$, $i_s(t)$ and $i_t(t)$, which depend only on the local average values of $\overline{v}_{cr}(t)$, $\overline{v}_{cs}(t)$ and $\overline{v}_{ct}(t)$, do not change. By the other side, the modification of voltages $\overline{v}_{cr}(t)$, $\overline{v}_{cs}(t)$ and $\overline{v}_{ct}(t)$ waveforms imply in altering the ripple current.

Fig. 3(b) shows the improvement in the current ripple (at the three phases), due to zero-sequence injection. At this point one can ask if there is an optimum value of $v_{0ref}(t)$ which can minimize, for instance, the harmonic content of the equivalent phase voltages (and, in consequence, of the resulting currents).

IV. PWM SPECTRA FOR ONE-PHASE AND THREE-PHASE CONVERTERS USING CPWM

Fig. 4 shows some PWM spectra, obtained by using computer simulation. Fig. 4(a) shows the spectrum of a HB converter with CPWM, with the carrier signal synchronized to the sinusoidal reference signal. The fundamental component appears at the reference frequency f_{ref} (harmonic order equal to 1 in Fig. 4(a)) with its amplitude proportional to the modulation index (considered here as the ratio between V_d and the peak value of v_{ref}), and the harmonics appear concentrated in bands centered on the carrier frequency f_S (harmonic order equal to 30 in Fig. 4(a)) and its integer multiples. The bands centered at f_S and its odd multiples have lower and upper sideband components with same amplitude and displaced by even multiples of the reference signal frequency f_{ref}. There are no even harmonics of the carrier frequency, but only bands centered around their positions, with lower and upper side components displaced by odd multiples of the reference signal frequency. These results can also be obtained analytically by using Bessel functions [1][2][8].

Fig. 4(b) shows the spectrum of a 3P3W converter using the same carrier for the three HB arms. It was shown [2] that the order of the symmetrical components in the neighborhood of the frequencies centered at the multiples of f_{ref} (Kf_{ref}), is as given by Fig. 5.

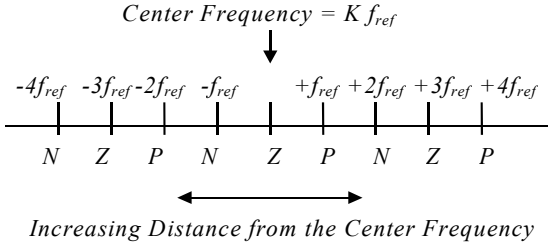

Fig. 5: Band components generated by a 3P3W converter at the neighborhood of the center frequency (Kf_{ref}). Z: zero sequence; P: positive sequence; N: negative sequence (from [2]).

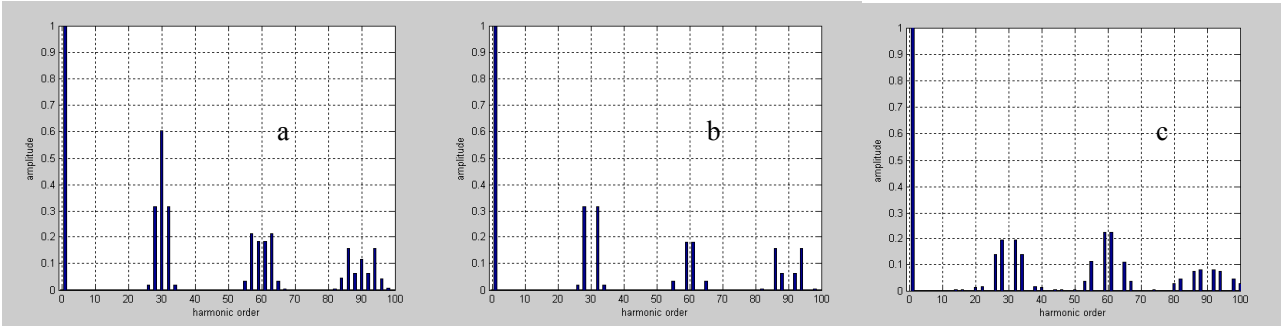

Fig. 4: Simulated PWM spectra: (a) v_C for an one-phase HB converter; (b) $\overline{v}_{cr}$ for a 3P3W converter; (c) $\overline{v}_{cr}$ for a 3P3W converter with instantaneous zero-sequence $v_0(t)$ injection. Simulation conditions: $V_d = 1\ p.u.$; $V_{ref} = 1\ p.u.$ (peak value) $f_S = 1/T_s = 30 \cdot f_{ref}$; $V_{0\,ref} = 0$ in spectra (a) and (b).

As the 3P3W has a three-wire load, the zero sequence components do not create currents at the load. The 30th harmonic high amplitude of a HB one-phase converter (Fig. 4(a)), does not appear in the spectrum of $\bar{v}_{cr}$ for a 3P3W (Fig. 4(b)), because it is a zero sequence component.

Fig. 4(c) shows the effect of applying an arbitrary zero-sequence $v_0(t)$ to the references. As described before, it modifies the resulting spectrum but the fundamental component is kept constant.

V. SPACE VECTOR PWM (SVPWM)

An alternative way for the analysis of three phase, three-wire systems is the use of the Space Vectors [5][7][10][11], where three-phase quantities (rst system) are mapped to a two dimensional system $\alpha\beta$, using (5a). The inverse transform is shown in (5b).

$$\vec{V} = \begin{bmatrix} v_a \\ v_b \end{bmatrix} = \frac{2}{3}\begin{bmatrix} 1 & -1/2 & -1/2 \\ 0 & \sqrt{3}/2 & -\sqrt{3}/2 \end{bmatrix}\begin{bmatrix} v_r \\ v_s \\ v_t \end{bmatrix} \quad (5a)$$

$$\begin{bmatrix} v_r \\ v_s \\ v_t \end{bmatrix} = \begin{bmatrix} 1 & 0 \\ -1/2 & \sqrt{3}/2 \\ -1/2 & -\sqrt{3}/2 \end{bmatrix}\begin{bmatrix} v_a \\ v_b \end{bmatrix} \quad (5b)$$

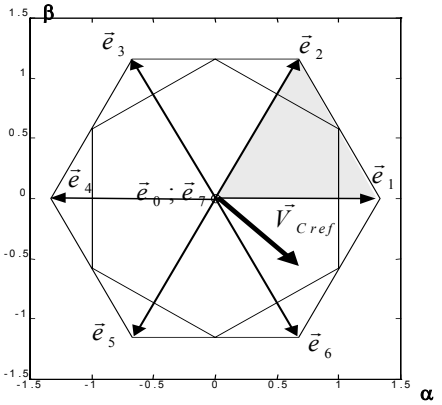

Fig. 6: Voltage Space Vectors $\vec{e}_i$ generated by the converter and the Locus of the synthesizable vectors $\vec{V}_{Cref}$

The SVPWM consists in generating the reference vector $\vec{V}_{Cref}$ (corresponding to the reference voltages $v_{r\_ref}, v_{s\_ref}, v_{t\_ref}$) as a convex combination of the voltage vectors generated by the converter $(\vec{e}_0, \vec{e}_1, \vec{e}_2, \vec{e}_3, \vec{e}_4, \vec{e}_5, \vec{e}_6, \vec{e}_7)$. At least three vectors are necessary to produce $\vec{V}_{Cref}$ [10][11]. The best choice is the triangular convex region that contains $\vec{V}_{Cref}$. In Fig.6, for example, the choice includes the two active vectors $\vec{e}_1, \vec{e}_6$ and the null vectors $\vec{e}_0, \vec{e}_7$. If the *i-th* vector is turned on for a time interval t_i, $\vec{V}_{Cref}$ can be written as a convex combination of $\vec{e}_1, \vec{e}_2, \vec{e}_0, \vec{e}_7$ (6).

$$\vec{V}_{Cref} = \frac{t_1}{T_s}\vec{e}_1 + \frac{t_2}{T_s}\vec{e}_2 + \frac{t_0}{T_s}\vec{e}_0 + \frac{t_7}{T_s}\vec{e}_7 = \\ = \alpha_1\vec{e}_1 + \alpha_2\vec{e}_2 + \alpha_0\vec{e}_0 + \alpha_7\vec{e}_7 = \alpha_1\vec{e}_1 + \alpha_2\vec{e}_2 \quad (6)$$

$$\alpha_1 + \alpha_2 + \alpha_0 + \alpha_7 = 1 \quad (7)$$

As $\vec{e}_0, \vec{e}_7$ are null, the vector equation (6) is a set of two scalar equations with two unknown variables α_1, α_2 Thus, the coefficients α_1, α_2 are easily calculated by solving (6). Using (7), the sum $(\alpha_0 + \alpha_7)$ is calculated by $(1 - \alpha_1 - \alpha_2)$. There are several possible choices for the sequence of imposed vectors [11]. Fig. 7 illustrates three cases. Fig. 7(a) requires two switching cycles per vector sequence $(\vec{e}_2, \vec{e}_1, \vec{e}_0)$. Fig. 7(b) produces two vector sequences $(\vec{e}_7, \vec{e}_2, \vec{e}_1, \vec{e}_0)$ or $(\vec{e}_0, \vec{e}_1, \vec{e}_2, \vec{e}_7)$ for two switching cycles, resulting in lower switching frequencies. Fig. 7(c) produces two vector sequences for three switching cycles, but is the option with lower current ripple, and is the sequence adopted for the SVPWM [10][11]. It is interesting to notice that this is exactly the sequence resulting from the CPWM, for a set of references $v_{r\_ref}, v_{s\_ref}, v_{t\_ref}$ that is equivalent to $\vec{V}_{Cref}$ (top of Fig. 3). The only unsolved question refers to the values of 'α_0, α_7'. Items VI and VII, and [10][11] show that imposing '$\alpha_0 = \alpha_7$' results in the lowest current ripple. From Fig. 4 one can notice that this condition is fulfilled if the maximum and minimum values of the set '$v_{r\_ref}, v_{s\_ref}, v_{t\_ref}$' have the same absolute value. This condition rarely happens for the CPWM, but can be easily accomplished by injecting an instantaneous zero sequence reference $v_{0\_ref\_SV}$ calculated by (8) [11]. For this condition the CPWM presents the same behavior as the SVPWM.

$$v_{0\_ref\_SV} = -\frac{\max(v_{r\_ref}, v_{s\_ref}, v_{t\_ref}) + \min(v_{r\_ref}, v_{s\_ref}, v_{t\_ref})}{2} \quad (8)$$

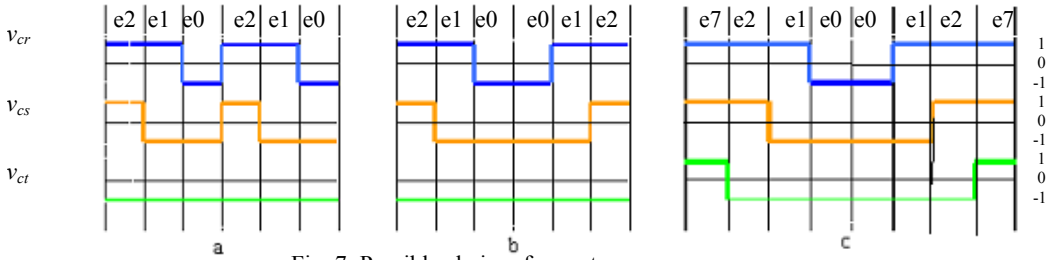

Fig. 7: Possible choices for vector sequence.

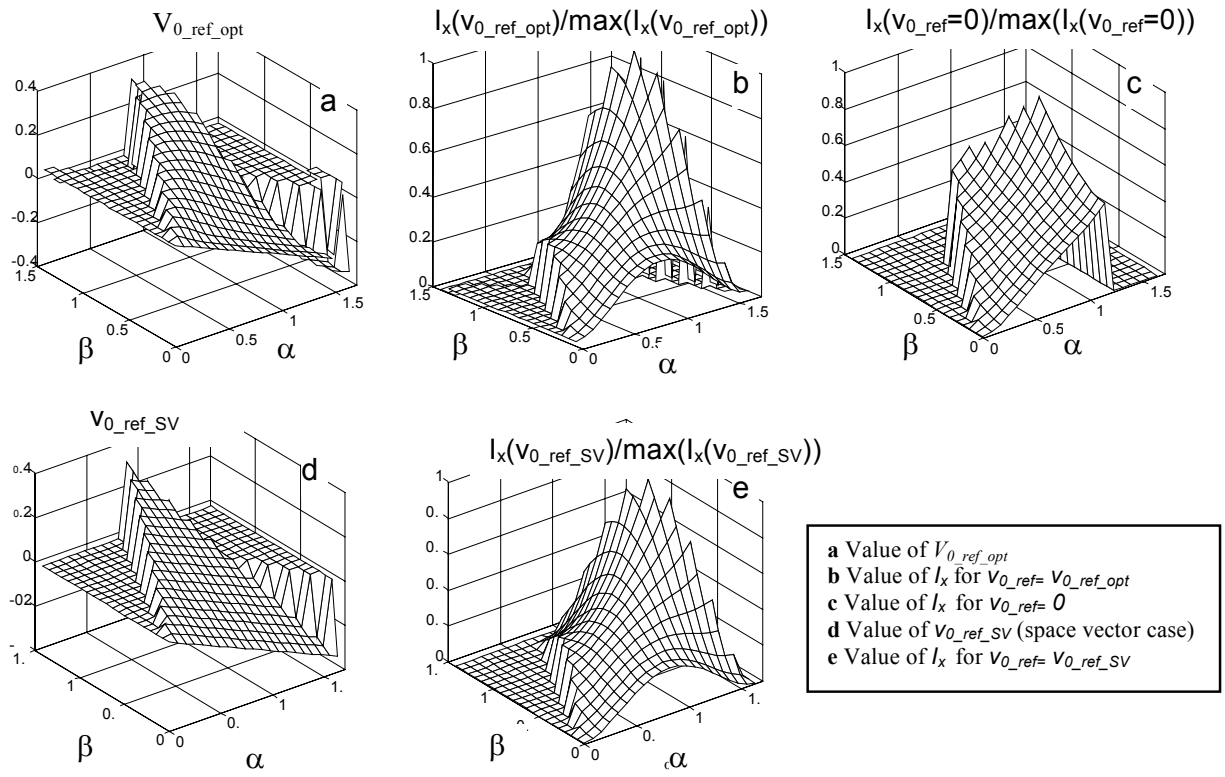

Fig. 8: Behavior of I_x for various values of the zero sequence reference signal v_{0_ref}

VI. OBTAINING THE OPTIMUM VALUE FOR THE ZERO SEQUENCE REFERENCE ($v_{0\_ref\_opt}$)

As shown in item III, the injection of a zero sequence signal v_{0_ref} to the reference signals ($v_{r\_ref}, v_{s\_ref}, v_{t\_ref}$) of the CPWM does not alter the averaged signal, but only the ripple currents [5][7]. A question immediately arises about the possibility of choosing an optimal value of v_{0_ref} that produces minimum current ripple. This problem can be treated as an optimization problem, where the cost function I_X is defined as the sum of the squared RMS values of the ripple phase currents, according to (10) [7].

$$I_x = \int_0^{Ts} (\Delta i_r{}^2 + \Delta i_s{}^2 + \Delta i_t{}^2)dt = \frac{v_{r\_ref}{}^2}{24} - \frac{5v_{r\_ref}{}^3}{72} + \frac{v_{r\_ref}{}^4}{24} + \frac{v_{r\_ref}v_{s\_ref}}{24} - \frac{5v_{r\_ref}{}^2 v_{s\_ref}}{48} + \frac{v_{r\_ref}{}^3 v_{s\_ref}}{12} + \frac{v_{s\_ref}{}^2}{24} - \frac{7v_{r\_ref}v_{s\_ref}{}^2}{48} + \frac{v_{r\_ref}{}^2 v_{s\_ref}{}^2}{8} - \frac{v_{s\_ref}{}^3}{18} + \frac{v_{r\_ref}v_{s\_ref}{}^3}{12} + \frac{v_{s\_ref}{}^4}{24} - \frac{3v_{r\_ref}{}^2 v_{s\_ref}v_{0\_ref}}{16} + \frac{3v_{r\_ref}v_{s\_ref}{}^2 v_{0\_ref}}{16} + \frac{v_{r\_ref}{}^2 v_{0\_ref}{}^2}{8} + \frac{v_{r\_ref}v_{s\_ref}v_{0\_ref}{}^2}{8} + \frac{v_{s\_ref}{}^2 v_{0\_ref}{}^2}{8} \quad (10)$$

As $v_{r\_ref} + v_{s\_ref} + v_{t\_ref} = 0$ (9), v_{t_ref} is written as a function of v_{r_ref} and. v_{s_ref}. The instantaneous zero sequence v_{0_ref} reference appears explicitly on (10). This equation is obtained from the current ripple waveforms of Fig. 4, by considering the load as three inductances with L=1H, $V_d = 1\,\mathrm{V}$ and $T_s = 1s$. The reference signals are considered constant during a switching period T_s.

For any given pair (v_{r_ref}, v_{s_ref}), the value $v_{0\_ref\_opt}$ that minimizes I_x is obtained by imposing that the partial derivative of I_x (11) is zero.

$$\frac{\partial I_x(v_{r\_ref}, v_{s\_ref}, v_{t\_ref}, v_{0\_ref})}{\partial v_{0\_ref}} = 0$$

$$\Rightarrow \quad v_{0\_ref\_opt} = \frac{3v_{r\_ref}v_{s\_ref}(v_{r\_ref} + v_{s\_ref})}{4(v_{r\_ref}{}^2 + v_{r\_ref}v_{s\_ref} + v_{s\_ref}{}^2)} \quad (11)$$

$v_{0\_ref\_opt}$ is plotted in Fig. 8(a), against the reference signals v_{r_ref}, v_{s_ref} and v_{t_ref}, represented here as a Space Vector $\vec{V}_{Cref}$ in the $\alpha\beta$ domain (Fig. 6). To improve the visualization of the graphics, only the gray colored part of the domain (Fig. 6) is used. Fig. 8(b) shows the value of I_x, when the $v_{0\_ref\_opt}$ is applied. Fig. 8(c) shows I_x for the original CPWM, without zero sequence injection. Substantial reduction of the ripple is achieved in Fig. 8(b) for reference signals, whose corresponding Space Vector ($\vec{V}_{Cref}$) is in the neighborhood of angles 0º, 60º, 120º, 180º, 240º and 300º of

the domain of $\vec{V}_{Cref}$ (Fig. 6). Small improvement is achieved near the angles 30°, 90°, 150°, 210°, 270° and 330°.

As explained in item V, the same behavior of the SVPWM can be obtained from the CPWM by injecting a zero sequence signal $v_{0\_ref\_SV}$ given by (8). Figs. 8(d) and 8(a) shows that $v_{0\_ref\_SV}$ and $v_{0\_ref\_opt}$ have similar shape. The same is valid for the value of I_x, for both $v_{0\_ref\_SV}$ and $v_{0\_ref\_opt}$ injection (Figs. 8(e), 8(b), 8(c)). These facts show that the SVPWM is nearly optimum according to the cost function I_x. It is easier to obtain the SVPWM behavior by injecting $v_{0\_ref\_SV}$ in a CPWM, than using the traditional method discussed in item V and [10][11]. Available dedicated DSPs provide good performance CPWM blocks, and (8) is easily calculated. The optimum PWM in (11) [7] presents no practical interest, because of its numerical complexity. Its importance lies on providing another way to show the optimal behavior of the SVPWM.

Some authors [4][6] showed the benefits of injecting third harmonic signals to the CPWM, presenting the optimum values for their amplitude and phase angle. It is clear now that these methods are somewhat limited, being restricted to sinusoidal, balanced set of references.

VII. CURRENT RIPPLE TRAJECTORY [9]

When generating a given reference vector $\vec{V}_{Cref}$, if the converter imposes the vector $\vec{e}_i$, the derivative of the ripple current vector due to $\vec{e}_i$ is given by "$\vec{D}_i = (\vec{e}_i - \vec{V}_{Cref})/L$"(12). Fig. 9(a) shows the vectors $\vec{D}_1;\vec{D}_2;\vec{D}_7;\vec{D}_0$, corresponding to vectors $\vec{e}_1,\vec{e}_2,\vec{e}_0,\vec{e}_7$. For the typical vector sequence of the CPWM $(\vec{e}_7,\vec{e}_2,\vec{e}_1,\vec{e}_0,\vec{e}_0,\vec{e}_1,\vec{e}_2,\vec{e}_7)$ the locus of the current ripple is shown in Fig. 9(b). For convenience, a rotating dq frame is attached do the reference vector $\vec{V}_{Cref}$. The lengths of the triangle sides are equal to $\left|\vec{D}_i t_i\right|$. As t_1,t_2 are uniquely defined by (6), the sides 1 and 2, and consequently the size of the triangle is defined by $\vec{V}_{Cref}$. The degree of freedom related to the choice of t_0,t_7, causes the variation of the lengths indexed by 0 and 7 at Fig. 9(b), forcing the two triangles to slide along the axis d. This shows why keeping $t_0 = t_7$ reduces the ripple along the axis d. No reduction can be achieved in axis q.

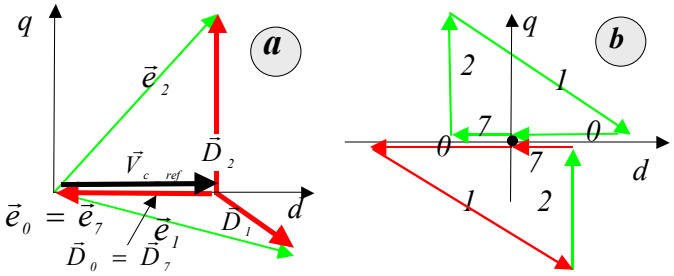

Fig.9: (a) converter voltage vectors and derivatives of the line current; (b) Locus of the current ripple vector

Simulation results for a set of sinusoidal, balanced PWM reference waveforms are shown in figure 10 for one period of the reference signals. The vector of the ripple current in the dq frame attached to $\vec{V}_{Cref}$ is shown for the original CPWM (Fig. 10(a)) and for the SVPWM (Fig. 10(b)). The improvement in the d axis is in the SVPWM.

VIII CONCLUSION

This paper joins information related to the comparison of the CPWM, SVPWM, CPWM with optimal zero sequence injection and CPWM with a zero sequence that emulates the SPWM behavior, with the purpose of deepening the understanding of CPWM and SVPWM strategies. It is emphasized that, in spite of their different origins, the SVPWM and CPWM emulating a SVPWM present exactly the same voltage and current waveforms. Optimum zero sequence reference is evaluated for the CPWM, showing that the SVPWM is a near optimum strategy considering the current ripple.

IX. REFERENCES

[1] H.S. Black, "Modulation Theory" Princetown, N.J., Van Nostrand & Co, 1953.

[2] T.L. Grant, T.H. Barton "Control Strategies for PWM

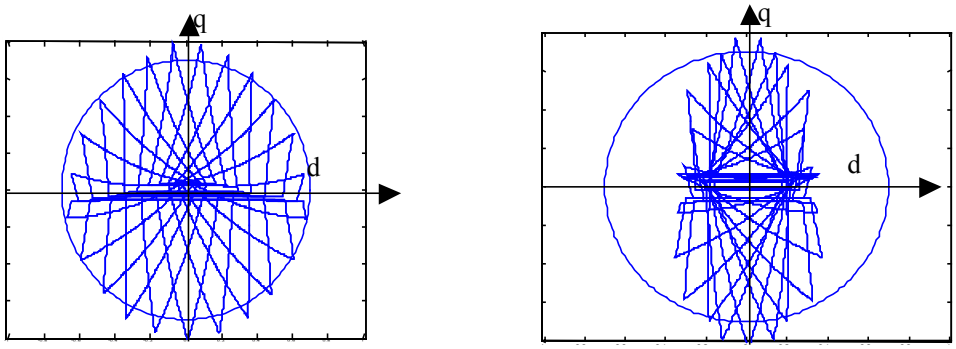

Fig. 10: Locus of the vector associated to the ripple current: (a) no zero sequence injection; (b) zero sequence injetion corresponding to the Space Vector PWM behavior

drives“. IEEE Transactions on Industrial Applications, Vol.16, Nº 2, pp. 211-215, March/April 1988.
[3] S.R. Bowes, “New sinusoidal pulsewidth-modulated invertor” Proc IEE, vol. 122, Nº11, November 1975.
[4] J.T. Boys and S.J. Walton, “A loss minimised sinusoidal PWM inverter“ IEE Proceedings, Vol. 132, Pt. B, Nº 5, September 1985.
[5] J. Holtz, “Pulsewidth Modulation – A Survey“ IEEE Transactions on Industrial Electronics, Vol.39, Nº5, October 1992.
[6] G.P. Sodermanns, “Methods of generating pulse patterns in voltage source P.W.M. inverters and implementation in an industrial drive“, EPE Aachen, 1989.
[7] L. Matakas Jr., E. Masada., “A instantaneous optimum PWM and its comparison to the space vector and regular sampling methods“, IEEJ94 Japan, 1994.
[8] J. Hamman, F.S. Van Der Merwe. “Voltage Harmonics Generated by Voltage-Fed Inverters Using PWM Natural Sampling“, IEEE Transactions on Power Electronics, Vol. 3, Nº 3, July 1988.
[9] I. Nagy, L. Matakas, Jr., E. Masada. “Novel adaptative switching pattern of AC-DC conversion for suppressing network pollution“, Third international conference on power quality: user applications and perspectives, October 24-27, 1994.
[10] H.W. Van Der Broeck, H.C. Skudelny, G.V. Stanke, “Analysis and realization of a pulse width modulator based on voltage space vectors”, IEEE Transactions on Industrial Applications, Vol.24, Nº 1, pp. 142-150, 1988.
[11] S. Buso. Lecture notes prepared for graduate classes at Campinas State University as invited professor - http://www.dsce.fee.unicamp.br/%7Eantenor/Simone2004.html.